ISBN: 978-3-95450-219-6 ISSN: 2226-0366 doi: 10.18429/JACoW-LINAC2024-MOPB029

AN ALTERNATIVE DESIGN SCHEME FOR CSNS-II MEBT DYNAMICS

Qiyu Kong*[1], Huachang Liu[1,2], Jun Peng[1,2]
Spallation Neutron Source Science Center, Dongguan, China
[1]also at Institute of High Energy Physics, Chinese Academy of Sciences (CAS), Beijing, China
[2]also at University of Chinese Academy of Sciences, Beijing, China

Abstract

The China Spallation Neutron Source (CSNS) has been operating at a stable beam power of 160 kW since March 2024, marking a significant 60% increase from its original design capacity. The ongoing CSNS upgrading project, known as CSNS-II. As part of this upgrade, a versatile Medium Energy Beam Transport (MEBT) system has been meticulously studied and redesigned to meet the stringent requirements for beam control in the presence of strong space charge effects. The MEBT system boasts several key functions and features, including beam chopping for optimizing beam structure, scrapers for confining and removing beam halo particles. Detailed studies on beam performance, in conjunction with the main linac, have been carried out and are presented in this article.

INTRODUCTION

The China Spallation Neutron Source (CSNS) leverages a high-energy proton accelerator to generate neutrons for a diverse array of scientific investigations [1]. The high-energy proton accelerator complex initiates with the 81 MeV H^- linear accelerator, consists of a 50 keV H^- ion source, a low energy beam transport line (LEBT), a 3 MeV Radio Frequency Quadrupole (RFQ), a medium energy beam transport line (MEBT), an 81 MeV Alvarez-type Drift Tube Linac (DTL) [2]. Then, H^- ion is stripping injected into rapid cycling synchrotron (RCS), where they are accelerated to 1.6 GeV.

The ongoing upgrade of the CSNS, known as CSNS-II, aims to enhance the linac peak current to 50 mA while the energy increase to 300 MeV, facilitated by a superconducting accelerator featuring Double-Spoke Resonators (DSR) [3] and Elliptical Resonators (EllipR). The layout of the linac in CSNS-II is illustrated in Fig. 1. Upon the successful completion of this upgrade, CSNS-II is poised to become the pioneering user open facility to deploy a superconducting linac as an RCS injector.

Table 1: The Main Parameters of the CSNS Linac in Phase-I and Phase-II

Parameter	Phase-I	Phase-II
Output energy (MeV)	81	300
Peak current (mA)	15	50
Repetition rate (Hz)	25	50
RF frequency (MHz)	324	324&648
Duty factor (%)	0.625	1.25

* kongqy@ihep.ac.cn

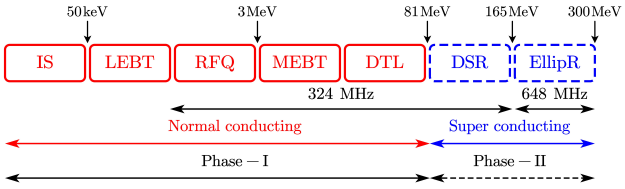

Figure 1: The layout of linac in CSNS-II.

The MEBT currently in operation at CSNS underwent joint commissioning with the DTL in 2018, at an energy level of approximately 3 MeV, which for high-intensity beam is a section dominated by space charge effect, making emittance growth seemingly inevitable. However, the functions it possesses are relatively simple and may not suffice to address the challenges posed by increased intensity, including emittance growth. In response to these evolving requirements, a series of research initiatives have been undertaken to develop a multi-functional MEBT dynamics scheme tailored to meet the demands of the CSNS-II project. This innovative approach aims to enhance the capabilities of the MEBT system to effectively manage emittance growth and other associated challenges arising from the intensified beam currents, thereby ensuring the continued success and optimal performance of the CSNS-II facility.

DESIGN PHILOSOPHY AND CONSIDERATIONS

In high-intensity accelerator facilities, the damage caused by beam losses due to various factors should be kept as low as possible along the linac, typically adhering to an acceptable threshold of 1 W/m for majority high-power particle accelerators [4]. Among all kinds of different possible beam loss sources in CSNS-II, the beam loss existing in MEBT or can be solved in MEBT mainly has the following three mechanisms:

- The linac in CSNS is equipped with a beam chopper at the LEBT with approximately a 20 ns rising edge [5]. It is important to note that the rising edge comprises several micro-pulses that are not entirely chopped.
- With CSNS-II operating at a beam current approximately five times higher than the existing facility, it is crucial to optimize beam halo at the entrance of the DTL.

CHOPPER SYSTEM

A pre-chopper in LEBT together with a chopper in MEBT is an effective solution to mitigate beam loss as in the SNS [6].

ISBN: 978-3-95450-219-6 ISSN: 2226-0366 doi: 10.18429/JACoW-LINAC2024-MOPB029

So, the new dynamics design of multi-functional MEBT in CSNS-II is considering adding a chopper. Typically, a chopper consists of two high-voltage electrode plates and a dump to absorb the chopped beam, as shown in Fig. 2. Here we define a kicker deflection angle α as follows to characterize the ability of the plate to deflect the particles:

$$\alpha = k\frac{V \cdot L}{G}, \quad (1)$$

where k is a coefficient, V is the plate voltage, L is the plate length, and G is the gap between two plates.

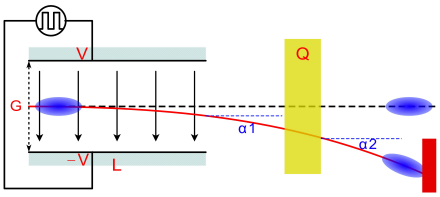

Figure 2: Configuration of a chopper system.

Basically, raising the plate voltage V and length L will increase the deflection angle but limited by the capabilities of the available electronic components and transverse envelope. Shortening the gap G will increase the electric field on the axis, but it should be large enough than beam size. Quadrupole Q could be inserted to achieve transverse matching. And the dipole field in the quadrupole will increase angle from $\alpha 1$ to $\alpha 2$.

The chopper has been build in TraceWin [7] for multiparticle tracking simulations. Particle density in chopper system is given in Fig. 3, beam is deflected to the -X direction under the electric field. The maximum value of the X-direction RMS envelope in the dynamics is about 2.5 mm, therefore, it is a relatively safe choice to choose the G of the plates at 20 mm.

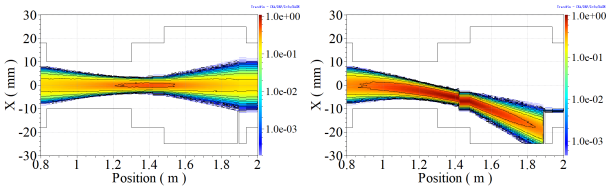

(a) Without chopper (b) With chopper

Figure 3: Particle density in chopper system.

Q for transverse matching is located at about 1.4 m as shown in Fig. 3, with a magnetic field gradient of 10.6 T/m. The dump of the chopper system is set at a distance of about 0.6 m from the exit of the plates and 11 mm away from the center axis.

A parameter scan of chopper voltage V was performed as shown in Fig. 4. Deflection angle α and proportion of particle lost in the dump were obtained under different V. The deflection angle $\alpha 1$ is approximately doubled due to Q's bipolar field. Particles are all lost in the dump when the voltage increases to ± 1750 V.

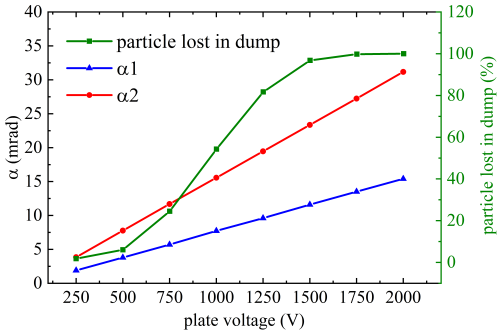

Figure 4: Deflection angle α and percentage of particles lost in the dump under different voltages.

SCRAPER SYSTEM

The physical design for the MEBT including chopper system was performed. As shown in Fig. 5, the MEBT can be divided into the chopper match section, the chopper section, and the DTL match section, consists of eight quadrupoles and two bunchers.

Two sets of scrapers are added to eliminate distortion phenomenon as shown in Fig. 6(a), one is located between Q1 and Q2, another is between Q5 and Q6. The phase advance between these two scrapers are about 90° and 60° in the horizontal and vertical plane, respectively. Each set of scrapers is capable of performing beam scraping in both the X and Y directions.

The effect of scrapers on beam performance have been investigated using multi-particle tracking simulation. We set the beam scraper radius in X and Y direction to be $R_{X/Y} = N \cdot \sigma_{X/Y}$, where $\sigma_{X/Y}$ is the RMS radius of the beam at the corresponding position of each beam scraper. Beam performance with different N are shown in Fig. 7. $N = 2.5 \sim 3$ can suppress the emittance growth and beam halo parameter H well, and the beam loss is within 3%, corresponding to a power deposition of less than 50 W. The phase space at the MEBT output with and without scrapers are given in Figs. 6(a) and 6(b), respectively.

END-TO-END SIMULATION

The end-to-end simulation results are presented below. Figure 8 show the evolution of beam density in transverse directions along the linac. Figure 9 shows the evolution of

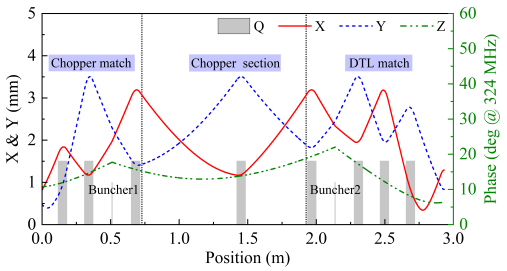

Figure 5: Elements layout and RMS envelope in upgraded MEBT.

ISBN: 978-3-95450-219-6 ISSN: 2226-0366 doi: 10.18429/JACoW-LINAC2024-MOPB029

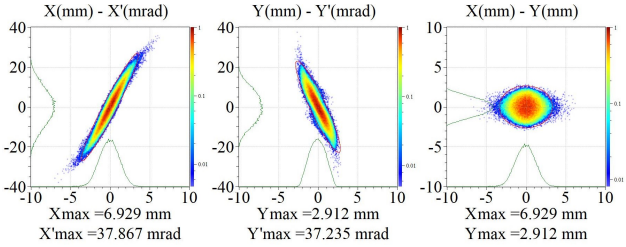

(a) Phase space at MEBT output without scrapers.

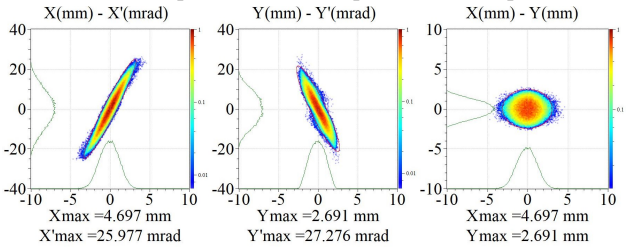

(b) Phase space at MEBT output with scrapers.

Figure 6: Phase space in upgraded MEBT.

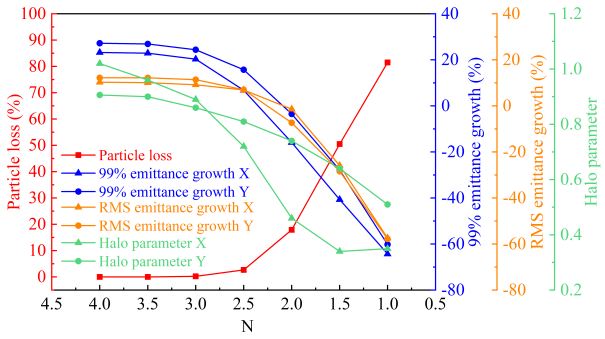

Figure 7: Beam performance with different N.

the RMS emittance through the linac, the RMS emittance growth were 18.9%/21.7%/3.5% at X/Y/Z direction.

The emittance growth $\varepsilon/\varepsilon_0$ for RMS, 99%, 99.9%, and 99.99% fractions with and without scrapers were gathered as shown in Fig. 10. Overall, the $\varepsilon/\varepsilon_0$ in all directions is suppressed by scrapers. Figure 11 gives the phase space distribution at the end of linac.

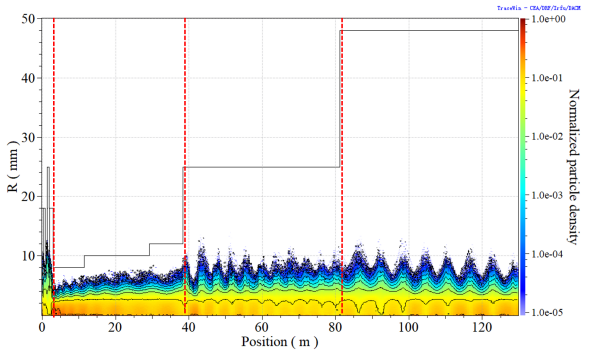

Figure 8: Transverse beam density along the linac. Four sections are MEBT, DTL, DSR, and EllipR, in order from left to right.

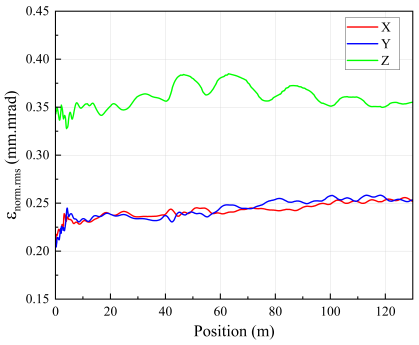

Figure 9: RMS emittance evolution along the linac.

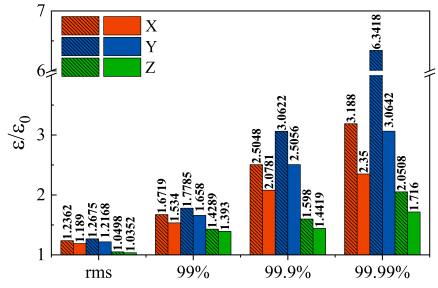

Figure 10: Emittance growth $\varepsilon/\varepsilon_0$ without and with scrapers through the linac for different fractions.

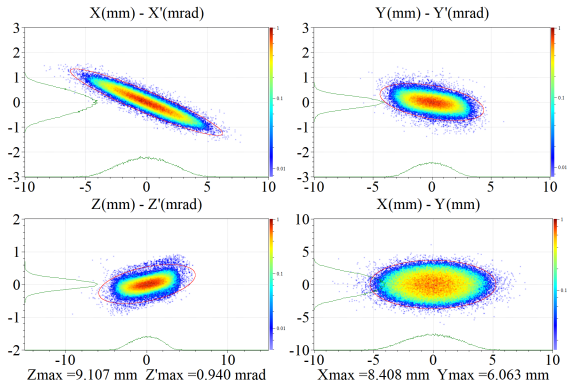

Figure 11: Phase space distribution at the end of linac.

SUMMARY

The beam dynamic design of the multi-functional MEBT system has been carefully conducted under the requirements of the CSNS-II. A new chopper section has been incorporated into the MEBT, physically feasible design scheme has been achieved within a limited longitudinal space. The design of scrapers has been strategically carried out within a reasonable phase shift interval to effectively remove halo particles both in X and Y directions. Approximately 3% particles are removed, resulting in a reduction of about 20% in transverse RMS emittance growth at the end of linac. With a total length of 2.9 m, it integrates various functions, meeting the stringent beam control requirements of the CSNS-II project.

ISBN: 978-3-95450-219-6 ISSN: 2226-0366 doi: 10.18429/JACoW-LINAC2024-MOPB029

REFERENCES

[1] W. Jie *et al.*, "China spallation neutron source - an overview of application prospects", *Chinese Physics C*, vol. 33, no. 11, p. 1033, Nov. 2009. doi:10.1088/1674-1137/33/11/021

[2] H. Liu *et al.*, "The design and construction of CSNS drift tube linac", *Nucl. Instrum. Methods*, vol. 911, p. 131–137, 2018. doi:10.1016/j.nima.2018.10.034

[3] W. Zhou *et al.*, "Development of the double spoke cavity prototype for CSNS-II", *Nucl. Instrum. Methods*, vol. 1062, p. 169170, 2024. doi:10.1016/j.nima.2024.169170

[4] Z.-J. Wang *et al.*, "Beam physics design of a superconducting linac", *Phys. Rev. Accel. Beams*, vol. 27, p. 010101, Jan. 2024. doi:10.1103/PhysRevAccelBeams.27.010101

[5] H. Liu *et al.*, "Design and experiment results of the LEBT pre-chopper for CSNS", *Nucl. Instrum. Methods*, vol. 654, pp. 2–7, 2011. doi:10.1016/j.nima.2011.04.035

[6] A. Aleksandrov and C. Deibele, "Experimental study of the SNS MEBT chopper performance", in *Proc. 1st Int. Particle Accelerator Conf. (IPAC'10)*, Kyoto, Japan, May. 2010, paper MOPD063, pp. 831–833.

[7] D. Uriot and N. Pichoff, "Status of TraceWin Code", in *Proc. 6th Int. Particle Accelerator Conf. (IPAC'15)*, Richmond, VA, USA, May. 2015, pp. 92–94. doi:10.18429/JACoW-IPAC2015-MOPWA008